Fatigue verification of high loaded bolts of a rocket combustion chamber.

Marcus Lehmann[1*] & Dieter Hummel[1]

[1] Airbus Defence and Space, Munich

Zusammenfassung

Rocket engines withstand intense thermal and structural loads. Either do the bolted interfaces between the engine components. Therefore particular emphasis is placed on quality assurance and verification by incoming inspection for fasteners. As part of the incoming inspection a fatigue test is performed to ensure high bolt durability covering the dynamic loads during engine operation. The difficulty is that a significant difference between test loads and flight loads exists which lead to a nonlinear relation between test results and expected operational life. To link both load cases a multi parametrical model is chosen and need to be adapted to both cases which is realized by a sensitivity analysis. While the parameters are scattered about the unifying parameter set also the life expectation varies for both load cases. Therefore a robustness analysis is finally performed to project the result variety under flight conditions onto the test result scattering.

Keywords: Bolt analysis, Robustness verification

*Kontakt: Airbus DS, 81663 München, Space Propulsion, Structure Mechanics & Design, E-Mail: marcus.lehmann@airbus.com

1 Introduction

Bolts or screws connect constructional parts with each other. The threaded bolt shaft and its evenly shaped counterpart, as nut or threaded blind hole, transmit forces by a shape-closed connection. In case of overloading the bolt will fail and thereby loose its force transmitting capability.

A bolt can be overloaded by overstressing which will lead to ductile failure, preferably at the first thread in contact. Another overloading mechanism is known as fatigue that becomes critical after a certain number of load cycles. The second is outlined in this paper.

2 Basics on bolt analysis

2.1 Pretension

During bolt mounting into a blind hole or a nut, pretension is to be generated. Continuous torque tightening increases the bolt force and the flange force in the same rate while the value of deformation depends on the stiffness of both components. Due to the tension load the bolt is strained by the law of elasticity $\Delta l_B = F_B/K_B$ with the bolt force F_B and the bolt's rigidity K_B that leads to the absolute bolt deformation Δl_B. With the same force F_B but with a different flange stiffness K_F the flange parts are compressed about

$\Delta l_F = F_B/K_F$. Here Δl_F denotes the deformation of the flange area in an imaginary cylinder between the bolt head and the nut. K_F is the corresponding flange stiffness.

The mounted and pre-stressed interface is loaded by the operational force F_L. If F_L is oriented in tension direction the bolt will be additionally stressed while the flange compression decreases. Hence the operational load is taken by both components in dependence from their stiffness. The ratio between the force fraction taken by flange decompression F_{LF} and the part covered by the bolt F_{LB} is defined by the force ratio Φ:

$$\Phi = \frac{K_B}{K_B + K_F} = \frac{F_{LB}}{F_L}. \tag{1}$$

The bolt and flange behaviour due to pretension and operational load are illustrated in figure 1.

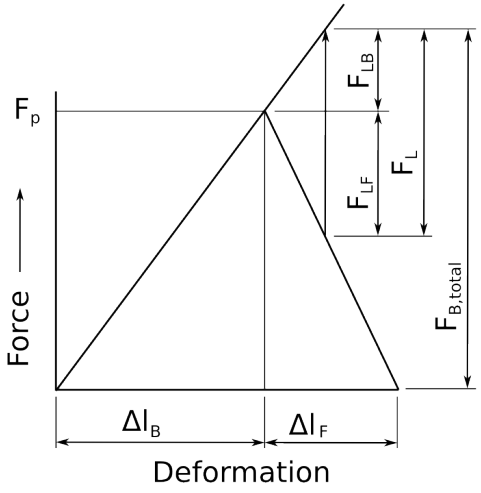

Figure 1: Load-deformation-curve of a classical bolt connection.

The effect of the force ratio becomes substantial for dynamic loading domains. The high durability of bolted joints is to be attributed to Φ and the fact that an operational load is partly taken by the relief of the prestressed flanges. The higher the flange stiffness is compared to the stiffness of the bolt shaft, the lower the actual impact of operational loads stresses the bolt. This effect can be seen in the relations of equ. (1). Due to this advantageous behaviour the bolts stress range per cycle is decreased which crucially increases bolt life.

2.2 Stress distribution

Loaded by an axial force F_{ax} the nominal stress σ_{nom} within the bolt shaft equals to:

$$\sigma_{nom} = \frac{F_{ax}}{A_{st}}, \tag{2}$$

with A_{st} as stress area.

Notch effects at the thread ground lead to a local stress concentration $\sigma_{max} = K \cdot \sigma_{nom}$. The stress concentration factor K depends beside others on the depth of the thread and the radius of the thread ground. To estimate the magnitude of K tables are presented in engineering literature, e.g. Young and Budynas [2002]. As result of the stress concentration at the thread grounds a stress distribution equivalent to figure 2 occurs.

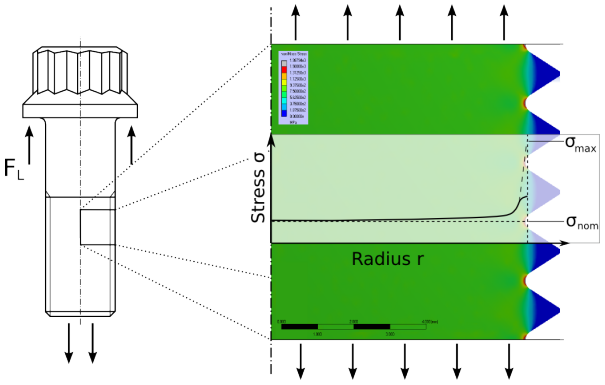

Figure 2: Stress distribution along threaded bolt. Stress concentration at thread grounds.

When the locally increased stress reaches the yield limit σ_y, local plastic deformations will occur. For the present study the Neuber rule is used to approximate the magnitude of plastic deformation the Neuber rule is used. Neuber expects a hyperbola in the stress-strain-field where the product of stress and

strain stays constant $\sigma\varepsilon = \sigma_{max}^2/E$. When the Neuber hyperbola fits the endpoint of the linear extrapolated stress-strain line $\sigma_{max,el}$, it will cross the yield curve at the point $\sigma_{max,Neuber}$. This point approximates the stress-strain relation after yielding. See figure 3 for visualisation. As yield curve a bilinear approximation is used. It is defined by the yield limit $(R_{p0.2}/E, R_{p0.2})$ and at ultimate conditions (A, R_M).

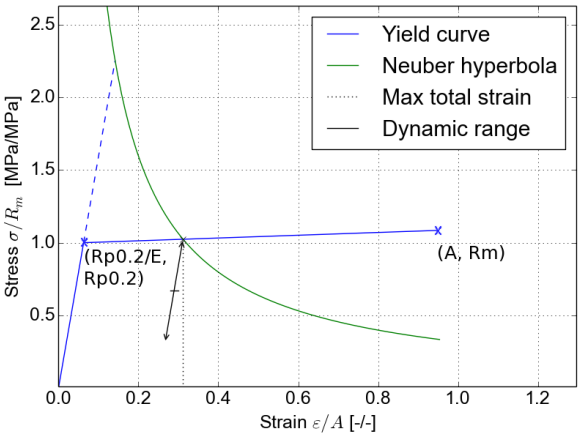

Figure 3: Plastic stress-strain state obtained by Neuber approximation.

2.3 Fatigue damage

The bolt life prediction is realized by the Coffin Manson approach. With the universal slope proposed by Lemaitre and Chaboche [1990]:

$$\Delta\varepsilon_{\text{univ.}} = f(N_f) = 3.5\frac{R_m - \sigma_m}{E} \cdot N_f^{-0.12} + D_u^{0.6} \cdot N_f^{-0.6} \quad (3)$$

the total strain range $\Delta\varepsilon$ is related to the number of cycles until failure N_f. R_m being the ultimate strength, D_u the ductility of the material and σ_m the mean stress of the load cycle.

Herein the values in the exponents are fitted to a wide range of different materials for universal validity. To reach our needs these constants are considered as material specific and are chosen in accordance to the bolt material. A better adjustable form of (3) is used with the parameters C_1 to C_4 that can be fit to actual material behaviour:

$$\Delta\varepsilon = f(N_f) = C_1\frac{R_m - \sigma_m}{E} \cdot N_f^{-C_2} + D_u^{C_3} \cdot N_f^{-C_4}. \quad (4)$$

Aligned values for C_1 to C_4 can be found for different materials in Lemaitre and Chaboche [1990]. Varying the constants C_1 to C_4 of (4) influence the $\Delta\varepsilon - N_f-$Curve as shown in figure 4. The actual sensitivity of the model towards these Coffin Manson parameters is analysed in section 4.

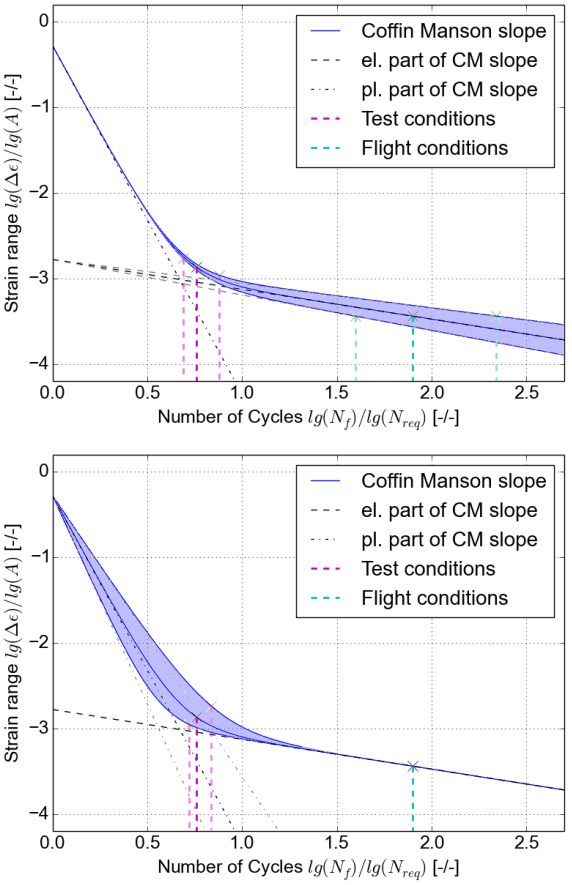

Figure 4: Coffin Mansons fatigue curve. Variety of the constants C_2 and C_4 are shown by the diffuse bluish areas.

3 Bolt validation procedure and uncertainties

To accept the bolts for flight application a few bolts per batch are submitted to several different test procedures. To check towards fatigue failure a cycling test is performed. It is shown that the load conditions during the test differ to those experienced during rocket launch. The objective of this investigation is to correlate the results of the fatigue test into the circumstances during flight. Finally it is to show that required cycles during flight can be validated by a certain number of test cycles.

3.1 Validation test conditions

For fatigue testing the bolt is inserted to the testing device with contact at thread and bolt head. No flange material is considered. Loads applied through the device are fully covered by the bolt itself. The full range of alternating testing loads is applied to the bolt. The diagram in figure 5a displays the load-deformation curve of this behaviour.

The large load range of $2F_a$ combined with the stress concentration factor at thread ground leads to local cyclic plastification as earlier shown in figure 2. According to the Neuber approximation this opens the stress-strain hysteresis, stretches the stress range and reduces the bolt life significantly.

3.2 Flight conditions

The considered bolts connect the combustion chamber to the injector. During mounting a high pretension F_p is applied to avoid interface sliding. The dynamic interface loads F_L occur in a moderate level which leads to relatively low alternating bolt force F_a compared to the pretension force F_p. The ratio can be seen in the load-deformation curve in figure 5b. With high flange stiffness, which is given in this case, the dynamic loads on-top to pretension are

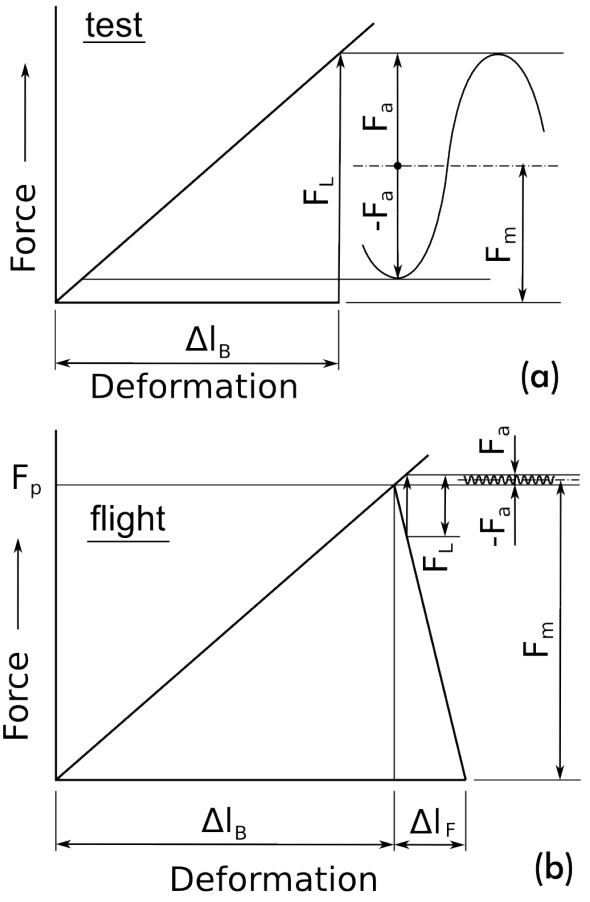

Figure 5: Load-deformation-curve under a) test conditions and b) flight conditions.

mostly covered by flange relief. The actual bolt load F_a alternates in a much smaller stress range compared to the test case. That leads to a solely elastic dynamic behaviour with a much smaller strain range. According to Coffin Manson and as seen in figure 4, a small $\Delta\varepsilon$-flight results in significant longer bolt life than under test conditions

3.3 Correlation of test results to flight conditions

To compare test result with flight live expectations the above mentioned influences need to be considered. Slight uncertainties of yield

stress $R_{p0,2}$ and strain at rupture A lead to contrary changes in the calculation of the strain range via the Neuber Approximation approach and spreads the resulting live expectation. Additional uncertainties occur by varying the Coffin Manson coefficients C_1 to C_4. Also the stress concentration factor of the threat K is not a definite value but depends on geometrical width ratio and the edge radius which is not definitely detectable. It is treated as variable during following investigations.

In the following life expectations will be calculated by considering a certain set of the mentioned variables. Each parameter set gives two results:

- $N_{f,test}$ – life expectation under test conditions and
- $N_{f,flight}$ – life expectation during flight.

Finally it is to show that the flight requirement is reached in any case. Which means for the model in any possible combination of input variables. Parameter combinations that lead to lower life expectation need to be excluded by the choice of test conditions.

4 Robustness under flight conditions

The entirety of variables that are influencing the bolt's life expectation is analysed. After performing a sensitivity analysis with optiSLang it occurred that the influence of the parameters varies from flight to test case. The test case shows the highest sensitivity to the Coffin Manson variables C_1 and C_2 that are responsible for the high cycle domain of the slope.

For the flight case these variables have a minor impact. Despite to its small strain range $\Delta\varepsilon_{\text{flight}}$ the sensitivity is mostly strength driven. $R_{p0.2}$ and R_m are the most influencing parameters in this case. Table 1 lists the sensitivities for both cases.

Table 1: Model sensitivity under test and flight conditions towards input parameters.

Parameter	unit	Test	Flight
A_m	[%]	0	1
E	$[^{MPa}/_{MPa}]$	0	0
K	[%]	1	4
$R_{p0.2}$	$[^{MPa}/_{MPa}]$	9	36
R_m	$[^{MPa}/_{MPa}]$	16	58
C_1	[%]	47	3
C_2	[%]	17	5
C_3	[%]	1	0
C_4	[%]	6	0

Considering the influencing parameters as normal distributed, the model is fed with specific parameter sets. The distribution of the parameters is evaluated from test data, or in the case of the Coffin Manson variables from literature. For each input set an output of the two life expectations is obtained - one for test and one for flight.

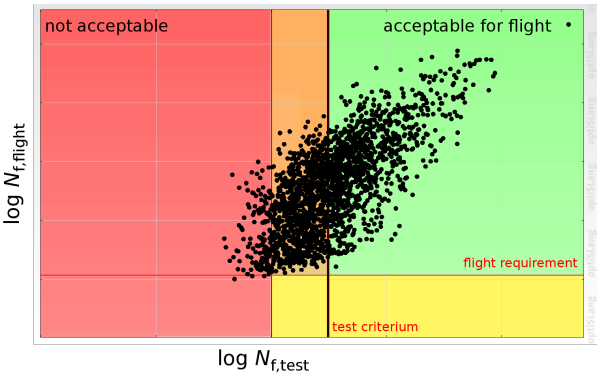

Figure 6: Criteria for fatigue test.

With the optiSLang software a robustness analysis was executed. As result of the life evaluation the plot in figure 6 is drawn. It shows the life results of 5000 parameter sets. For each set the expected flight life is prognosed for an calculated test life. As requirement for flight acceptance the bolts have to withstand

the specified loads, even with the worst possible combination of material parameters. To speak in colours regarding figure 6 all points below the flight requirements must not be accepted. That means all test results in the red area will lead to bolt rejection from flight worthiness. If one of the few tested bolts per incoming batch shows an unacceptable fatigue durability the whole batch will not be mounted.

The actual test requirement is finally defined at a higher number of cycles during test to meet an additional safety factor. Test results in the orange area can achieve acceptance level by performing additional analysis. The big plus of the indifferent orange area is the early recognition of any disadvantegeous changes of production methods. If processes change the final product may be affected in a negative way. With the demanding test requirement changes can early be detected and counteractions can be prepared.

The bolts that meet the test requirement, illustrated by the green area in the plot, are accepted for flight without further analysis.

The acceptance regarding bolt life could finally be verified. With the possibility of taking all parameters into account within a single analysis, the understanding of its sensitivities was improved. Having the bandwidth of each parameter in mind the spread of the bolt life expectation was shown. In the anthill plot this life expectation was projected on the durability under testing conditions. With the relations between flight and test a new test criteria was found that disqualifies unacceptable bolts before they go to flight.

Literature

Jean Lemaitre and Jean-Louis Chaboche. *Mechanics of solid materials*. Cambridge university press, 1990.

Warren Clarence Young and Richard Gordon Budynas. *Roark's formulas for stress and strain*, volume 7. McGraw-Hill New York, 2002.